BULLETIN OF THE POLISH ACADEMY OF SCIENCES
TECHNICAL SCIENCES, Vol. 67, No. 5, 2019
DOI: 10.24425/bpas.2019.128652

Trajectory tracking and collision avoidance for the formation of two-wheeled mobile robots

W. KOWALCZYK* and K. KOZŁOWSKI

Poznan University of Technology, ul. Piotrowo 3A, 60-965 Poznan, Poland

Abstract. This paper presents control method for multiple two-wheeled mobile robots moving in formation. Trajectory tracking algorithm from [7] is extended by collision avoidance, and is applied to the different type of formation task: each robot in the formation mimics motion of the virtual leader with a certain displacement. Each robot avoids collisions with other robots and circular shaped, static obstacles existing in the environment. Artificial potential functions are used to generate repulsive component of the control. Stability analysis of the closed-loop system is based on Lyapunov-like function. Effectiveness of the proposed algorithm is illustrated by simulation results.

Key words: robot formation, nonholonomic robot, stability analysis, Lyapunov-like function, path following, artificial potential function.

1. Introduction

First works concerning the problem of collision avoidance in multiagent system were published by Laitmann and Skowronski in 1977 [1] and 1980 [2]. They investigated control of two agents avoiding collisions with each other. In 1986 Khatib proposed new control algorithm [4] in which he combined attracting (to the goal) and repelling (from the obstacles) interactions. The novelty was the use of artificial potential functions (APF), similar to models of intermolecular interactions. The control is based on the gradient of combined attracting APF and one or more (depending on the number of obstacles present in the neighbourhood of the robot) repelling APFs. This method was computationally effective and even in the 1980s could provide real-time response. This property resulted in great popularity of this concept. Currently it is widely used in the control of multi-robot systems.

Alternative approach is method based on game theory. Authors of [20] propose two-step methodology for the group of unicycle robot. In the first step, exploiting a differential game formulation, collision-free trajectories are generated for virtual agents. At this stage robots are modelled as single integrator. In second step the previous step is used to construct dynamic feedback strategies for the wheeled mobile robots which guarantee that the robots reach their targets avoiding collisions. Game theoretic concept combined with fuzzy-logic controller is proposed in [21] to solve collision free target tracking problem of multi-agent robot system. In paper [22] game theory approach is adopted to minimize the time needed by the two robots to deploy sensor nodes in an area containing obstacles.

In recent years a lot of articles in dealing with the subject of multiple mobile robot control have been published, based on the kinematic model of the mobile platforms [8, 19], and the ones considering their dynamic properties [3, 18]. Many algorithms for multi-robot systems based on the navigation function (NF) have been also proposed [11–15]. NF approach removes the problem of local minima [16, 17], however, its computational complexity causes that it is not often used in practice.

This paper presents control algorithms for a group of differentially driven mobile robots moving in formation. They execute trajectory tracking task. The algorithm is based on the paper [7]; it is extended with collision avoidance, and applied to the different type of task. Section 2 presents formulation of the problem. Section 3 describes control algorithm for the formation of non-holonomic mobile robots. In Section 4 stability analysis is given. Simulation results are presented in Section 5. In the last Section concluding remarks are given.

2. Problem description

The task of the formation is to follow virtual leader that moves with desired linear and angular velocities $[v_l, \omega_l]^T$. The kinematic model of the i-th differentially-driven mobile robot R_i ($i = 1 \ldots N$, N – number of robots) is given by the following equation:

$$\dot{q}_i = \begin{bmatrix} \cos\theta_i & 0 \\ \sin\theta_i & 0 \\ 0 & 1 \end{bmatrix} u_i \tag{1}$$

where vector $q_i = [x_i \ y_i \ \theta_i]^\top$ denotes the pose and x_i, y_i, θ_i are position coordinates and orientation of the robot with respect to a global, fixed coordinate frame. Vector $u_i = [v_i \ \omega_i]^\top$ is the control vector with v_i denoting linear velocity control and ω_i denoting angular velocity control of the platform.

The robots are expected to imitate the motion of the virtual leader. They should have the same velocities as the virtual

*e-mail: wojciech.kowalczyk@put.poznan.pl

Manuscript submitted 2019-01-27, revised 2019-04-05, initially accepted for publication 2019-04-20, published in October 2019

leader. The position coordinates $[x_l \;\; y_l]^T$ of the virtual leader are used as a reference position for the individual robots but each of them have different spatial displacement with respect to the leader:

$$\begin{aligned} x_{id} &= x_l + d_{ix} \\ y_{id} &= y_l + d_{iy}, \end{aligned} \tag{2}$$

where vector $[d_{ix} \;\; d_{iy}]^T$ is desired displacement of the i-th robot. As the robots position converge to the desired values their orientations θ_i converge to the orientation of the virtual leader θ_l. Figure 1 presents formation of four robots tracking desired trajectory without error.

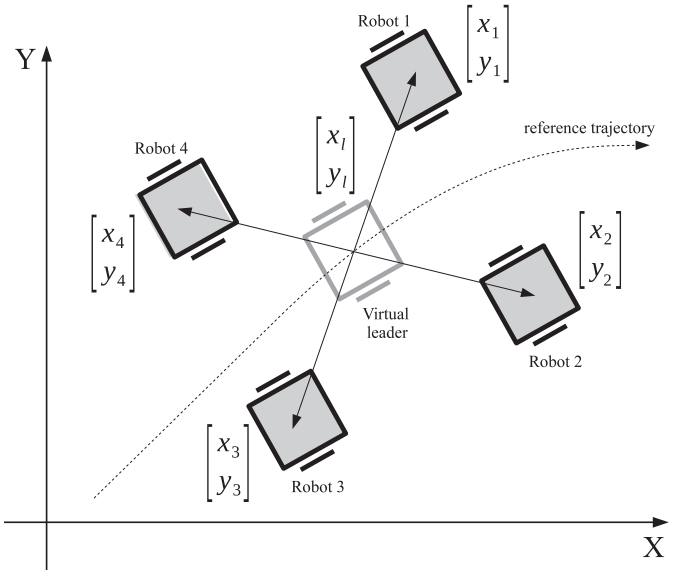

Fig. 1. Formation of four robots tracking desired trajectory without error. Arrows pointing from the virtual leader to the robots represent displacements $[d_{ix} \;\; d_{iy}]^T$

3. Control algorithm

The goal of the control is to drive the formation along the desired trajectory avoiding collisions between agents and other obstacles. Achieving control goals is equivalent to bringing the following quantities to zero:

$$\begin{aligned} p_{ix} &= x_{id} - x_i \\ p_{iy} &= y_{id} - y_i \\ p_{i\theta} &= \theta_l - \theta_i. \end{aligned} \tag{3}$$

Assumption 1. $\forall\{i,j\},\ i \neq j,\ \left\|[x_{id} \;\; y_{id}]^T - [x_{jd} \;\; y_{jd}]^T\right\| > R_j.$

Assumption 2. If robot i gets into avoidance region of any other robot/obstacle $j, j \neq i$ its desired trajectory is temporarily frozen ($\dot{x}_{id} = 0, \dot{y}_{id} = 0$). If the robot leaves the avoidance area its desired coordinates are immediately updated. As long as the robot remains in the avoidance region its desired coordinates are periodically updated at certain discrete instants of time. The time period t_u of this update process is relatively large in comparison to the main control loop sample time.

Assumption 1 comes down to the statement that desired paths of individual robots are planned in such a way that is steady state all robots are outside of the collision avoidance regions of other robots/obstacles.

Assumption 2 means that tracking process is temporarily suspended because collision avoidance has a higher priority. Once the robot is outside the collision detection region, it updates the reference to the new values. In addition when the robot is in the collision avoidance region its reference is periodically updated. This low-frequency process supports leaving the unstable equilibrium points that occur, e.g. when one robot is located exactly between the other robots and its goal.

The system error expressed with respect to the coordinate frame fixed to the robot is described below:

$$\begin{bmatrix} e_{ix} \\ e_{iy} \\ e_{i\theta} \end{bmatrix} = \begin{bmatrix} \cos\theta_i & \sin\theta_i & 0 \\ -\sin\theta_i & \cos\theta_i & 0 \\ 0 & 0 & 1 \end{bmatrix} \begin{bmatrix} p_{ix} \\ p_{iy} \\ p_{i\theta} \end{bmatrix}. \tag{4}$$

Using the above equations and non-holonomic constraint $\dot{y}_i \cos(\theta_i) - \dot{x}_i \sin(\theta_i) = 0$ the error dynamics between the leader and the follower are as follows:

$$\begin{aligned} \dot{e}_{ix} &= e_{iy}\omega_i - v_i + v_l \cos e_{i\theta} \\ \dot{e}_{iy} &= -e_{iy}\omega_i + v_l \sin e_{i\theta} \\ \dot{e}_{i\theta} &= \omega_l - \omega_i. \end{aligned} \tag{5}$$

Collision avoidance behaviour is based on the artificial potential functions (APF). This concept originally was proposed in [4]. All robots are surrounded by APFs that raise to infinity near objects border r_j (j – number of the robot/obstacle) and decreases to zero at some distance R_j, $R_j > r_j$.

One can introduce the following function [9]:

$$B_{aij}(l_{ij}) = \begin{cases} 0 & \text{for} \quad l_{ij} < r_j \\ e^{\frac{l_{ij} - r_j}{l_{ij} - R_j}} & \text{for} \quad r_j \leq l_{ij} < R_j \\ 0 & \text{for} \quad l_{ij} \geq R_j \end{cases}, \tag{6}$$

that gives output $B_{aij}(l_{ij}) \in \langle 0,1)$. Distance between the i-th and the j-th robot is defined as the Euclidean length $l_{ij} = \left\|[x_j \;\; y_j]^\top - [x_i \;\; y_i]^\top\right\|$.

Scaling the function given by Equation (6) within the range $\langle 0, \infty)$ can be given as follows:

$$V_{aij}(l_{ij}) = \frac{B_{aij}(l_{ij})}{1 - B_{aij}(l_{ij})}, \tag{7}$$

that is used later to avoid collisions.

In further description terms 'collision area' or 'collision region' is used for locations fulfilling conditions $l_{ij} < r_j$. The range $r_j < l_{ij} < R_j$ is called 'collision avoidance area' or 'collision avoidance region'.

One can introduce the position correction variables that consist of position error and collision avoidance terms:

$$\begin{aligned} P_{ix} &= p_{ix} - \hat{w}_{ix} \\ P_{iy} &= p_{iy} - \hat{w}_{iy}, \end{aligned} \tag{8}$$

where

$$\hat{w}_{ix} = \sum_{j=1, j\neq i}^{N+M} \hat{w}_{ijx}, \quad \hat{w}_{iy} = \sum_{j=1, j\neq i}^{N+M} \hat{w}_{ijy}$$

are components of the consolidated collision avoidance vector $\hat{w}_i = [\hat{w}_{ix} \;\; \hat{w}_{iy}]^T$, and

$$\hat{w}_{ijx} = \frac{\partial V_{aij}}{\partial x_i}, \quad \hat{w}_{ijy} = \frac{\partial V_{aij}}{\partial y_i}$$

are components of the j-th obstacle APF's gradient $\hat{w}_{ij} = [\hat{w}_{ijx} \;\; \hat{w}_{ijy}]^T$ with respect to the global coordinate frame computed in the location of the i-th robot (Fig. 2), M – number of static obstacles. V_{aij} depends on x_i and y_i according to Equation 7. It is assumed that robots avoid collisions with each other and other obstacles present in the taskspace (only circle-shaped can occur). The correction variables are transformed to the local coordinate frame fixed in the mass centre of the robot:

$$\begin{bmatrix} E_{ix} \\ E_{iy} \\ e_{i\theta} \end{bmatrix} = \begin{bmatrix} \cos\theta_i & \sin\theta_i & 0 \\ -\sin\theta_i & \cos\theta_i & 0 \\ 0 & 0 & 1 \end{bmatrix} \begin{bmatrix} p_{ix} \\ p_{iy} \\ p_{i\theta} \end{bmatrix}. \tag{9}$$

Differentiating first two equations of (3) with respect to the p_{ix} and p_{iy} respectively one obtains:

$$\begin{aligned} \frac{\partial x_i}{\partial p_{ix}} &= -1 \\ \frac{\partial y_i}{\partial p_{iy}} &= -1. \end{aligned} \tag{10}$$

Using (10) one can write:

$$\begin{aligned} \frac{\partial V_{aij}}{\partial p_{ix}} &= \frac{\partial V_{aij}}{\partial x_i}\frac{\partial x_i}{\partial p_{ix}} - \frac{\partial V_{aij}}{\partial x_i} \\ \frac{\partial V_{aij}}{\partial p_{iy}} &= \frac{\partial V_{aij}}{\partial y_i}\frac{\partial y_i}{\partial p_{iy}} - \frac{\partial V_{aij}}{\partial x_y}. \end{aligned} \tag{11}$$

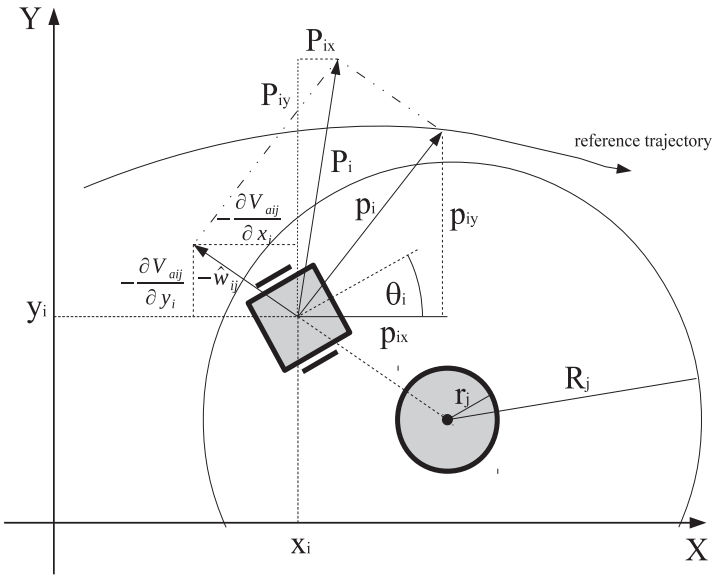

Fig. 2. Robot in the environment with obstacle (details expressed in the global coordinate frame)

Taking into account Equations 8 and 9 gradient of the APF can be expressed with respect to the local coordinate frame fixed to the i-th robot:

$$\begin{bmatrix} \frac{\partial V_{aij}}{\partial e_{ix}} \\ \frac{\partial V_{aij}}{\partial e_{iy}} \end{bmatrix} = \begin{bmatrix} \cos\theta_i & \sin\theta_i \\ -\sin\theta_i & \cos\theta_i \end{bmatrix} \begin{bmatrix} \frac{\partial V_{aij}}{\partial p_{ix}} \\ \frac{\partial V_{aij}}{\partial p_{iy}} \end{bmatrix}. \tag{12}$$

Equation 12 can be verified easily taking into account inverse transformation of the first two equations of (4) and by taking partial derivatives of $V_{aij}(d_{ix} - p_{ix}, d_{iy} - p_{iy}) = V_{aij}\big(d_{ix} - p_{ix}(e_{ix}, e_{iy}), d_{iy} - p_{iy}(e_{ix}, e_{iy})\big)$.

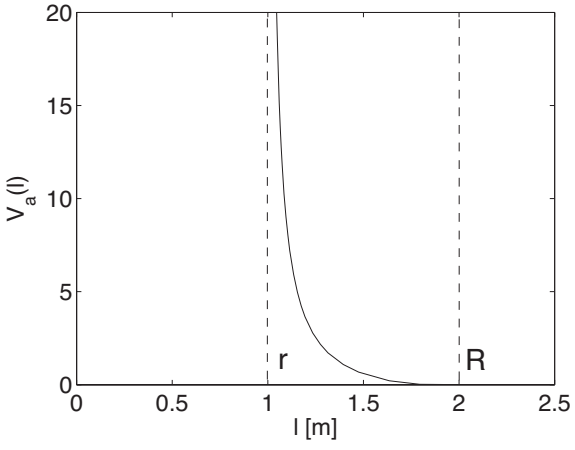

Fig. 3. APF as a function of distance to the centre of the robot (indexes omitted for simplicity)

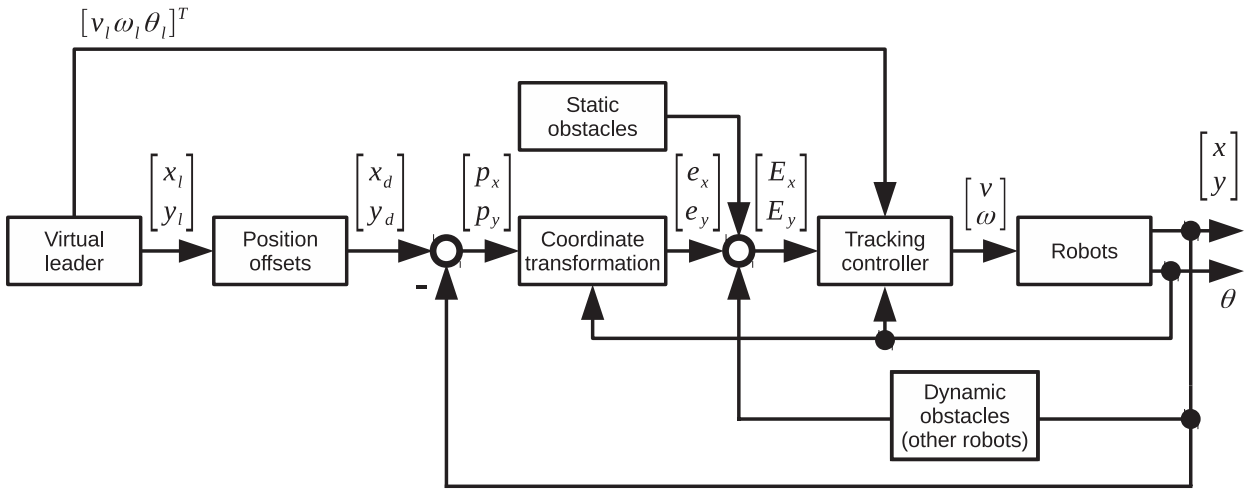

Fig. 4. Schematic diagram of the MIMO control system

Using (11) above equation can be written as follows:

$$\begin{bmatrix} \dfrac{\partial V_{aij}}{\partial e_{ix}} \\ \dfrac{\partial V_{aij}}{\partial e_{iy}} \end{bmatrix} = \begin{bmatrix} -\cos\theta_i & -\sin\theta_i \\ \sin\theta_i & -\cos\theta_i \end{bmatrix} \begin{bmatrix} \dfrac{\partial V_{aij}}{\partial x_i} \\ \dfrac{\partial V_{aij}}{\partial y_i} \end{bmatrix}. \tag{13}$$

Equation 9 using (8) and (13) can be transformed to the following form:

$$\begin{aligned} E_{ix} &= p_{ix}\cos(\theta_i) + p_{iy}\sin(\theta_i) + w_{ix} \\ E_{iy} &= -p_{ix}\sin(\theta_i) + p_{iy}\cos(\theta_i) + w_{ix} \\ e_{i\theta} &= p_{i\theta} \end{aligned} \tag{14}$$

where

$$w_{ix} = \sum_{j=1, j\neq i}^{N+M} w_{ijx}, \quad w_{iy} = \sum_{j=1, j\neq i}^{N+M} w_{ijy} \tag{15}$$

are components of the consolidated collision avoidance vector $w_i = [w_{ix} \;\; w_{iy}]^T$, and

$$w_{ijx} = \frac{\partial V_{aij}}{\partial e_{ix}}, \quad w_{ijy} = \frac{\partial V_{aij}}{\partial e_{iy}} \tag{16}$$

are components of the j-th obstacle APF's gradient $w_{ij} = [w_{ijx} \;\; w_{ijy}]^T$ with respect to the local coordinate frame (fixed to the robot) computed in the location of the i-th robot.

Each derivative of the APF is transformed from the global coordinate frame to the local coordinate frame fixed to the robot. Finally, correction variables expressed with respect to the local coordinate frame are as follows:

$$\begin{aligned} E_{ix} &= e_{ix} + w_{ix} \\ E_{iy} &= e_{iy} + w_{iy}. \end{aligned} \tag{17}$$

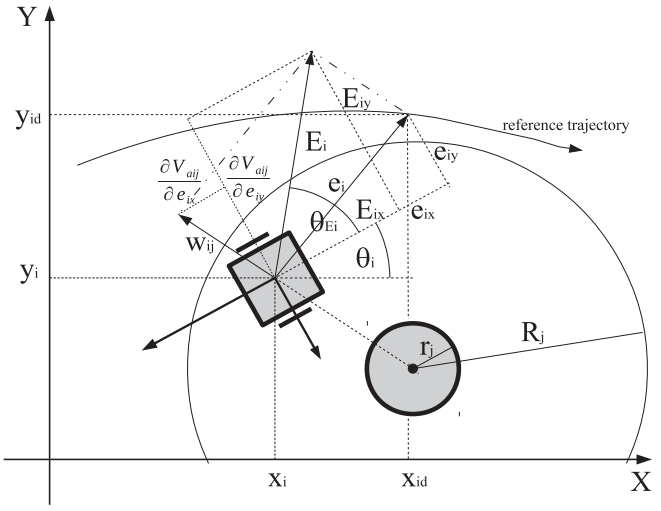

Fig. 5. Robot in the environment with obstacle

Note the similarity of the structure of Equations 8 (updated by Equation 11 and 17).

Figure 4 presents schematic diagram of the MIMO control system. It shows the general concept of the system's operation and the flow of the information between the subsystems. The following signals are marked:

$$[x \;\; y]^T = [x_1 \ldots x_N \;\; y_1 \ldots y_N]^T$$

$$\theta = [\theta_1 \ldots \theta_N]^T$$

that represent aggregated vectors of robot's coordinates; vector of aggregated desired coordinates:

$$[x_d \;\; y_d]^T = [x_{1d} \ldots x_{Nd} \;\; y_{1d} \ldots y_{Nd}]^T$$

vector of aggregated controls:

$$[v \;\; \omega]^T = [v_1 \ldots v_N \;\; \omega_1 \ldots \omega_N]^T$$

vectors of aggregated position errors expressed in global and local coordinate frame:

$$[p_x \;\; p_y]^T = [p_{1x} \dots p_{Nx} \;\; p_{1y} \dots p_{Ny}]^T$$

$$[e_x \;\; e_y]^T = [e_{1x} \dots e_{Nx} \;\; e_{1y} \dots e_{Ny}]^T$$

and vector of aggregated correction variables:

$$[E_x \;\; E_y]^T = [E_{1x} \dots E_{Nx} \;\; E_{1y} \dots E_{Ny}]^T.$$

Control algorithm from [7] for N robots extended by the collision avoidance is as follows:

$$\begin{aligned} v_i &= v_l + c_2 E_{ix} \\ \omega_i &= \omega_l + h(t, E_{iy}) + c_1 e_{i\theta} \end{aligned} \tag{18}$$

where $h(t, E_{iy})$ is bounded, depends linearly on E_{iy}, and continuously differentiable function. It must be properly chosen to ensure persistent excitation of the reference angular velocity [6]. Positive constants c_1 and c_2 are design parameters.

Assumption 3. If the value of the linear control signal v_i is less then considered threshold value $|v_i| < v_t$ (v_t – positive constant), it is replaced by a new value $\tilde{v}_i = S(v_i)v_t$, where

$$S(v_i) = \begin{cases} -1 & for \quad v_i < 0 \\ 1 & for \quad v_i \geq 0 \end{cases}. \tag{19}$$

By partial substitution of (18) into (5) one can express error dynamics as follows:

$$\begin{aligned} \dot{e}_{ix} &= e_{iy}\omega_i - c_2 E_{ix} + v_l(\cos e_{i\theta} - 1) \\ \dot{e}_{iy} &= -e_{ix}\omega_i + v_l \sin e_{i\theta} \\ \dot{e}_{i\theta} &= -h_i(t, E_{iy}) - c_1 e_{i\theta}. \end{aligned} \tag{20}$$

The above formula will be used in the stability analysis (Section 4).

Transforming (20) using (18) and taking into account Assumption 2 (when robot gets into collision avoidance region, velocities v_l and ω_l are replaced with 0 value) error dynamics can be expressed in the following form:

$$\begin{aligned} \dot{e}_{ix} &= h_i(t, E_{iy})e_{iy} + c_1 e_{iy} e_{i\theta} - c_2 E_{ix} \\ \dot{e}_{iy} &= -h_i(t, E_{iy})e_{ix} - c_1 e_{i\theta} e_{ix} \\ \dot{e}_{i\theta} &= -h_i(t, E_{iy}) - c_1 e_{i\theta}. \end{aligned} \tag{21}$$

4. Stability of the system

In this section stability analysis of the closed-loop system will be presented. When robots are outside of collision avoidance regions of other robots/obstacles (APF takes the value zero) the analysis given in [7] is actual and will be no repeated here.

Further the analysis for the situation in which the i-th robot is in the collision region of other robot is presented.

Consider the following Lyapunov-like function:

$$V = \sum_{i=1}^{N} \left[\frac{1}{2}(e_{ix}^2 + e_{iy}^2 + e_{i\theta}^2) + \sum_{j=1, j\neq i}^{N+M} V_{aij} \right]. \tag{22}$$

If robots are in the collision avoidance regions of other robots, time derivative of the Lyapunov-like function is calculated as follows:

$$\begin{aligned} \frac{dV}{dt} &= \sum_{i=1}^{N} \left[e_{ix}\dot{e}_{ix} + e_{iy}\dot{e}_{iy} + e_{i\theta}\dot{e}_{i\theta} + \right. \\ &\left. + \sum_{j=1, j\neq i}^{N+M} \left(\frac{\partial V_{aij}}{\partial e_{ix}}\dot{e}_{ix} + \frac{\partial V_{aij}}{\partial e_{iy}}\dot{e}_{iy} \right) \right] = \\ &= \sum_{i=1}^{N} \left[e_{ix}\dot{e}_{ix} + e_{iy}\dot{e}_{iy} + e_{i\theta}\dot{e}_{i\theta} + \right. \\ &\left. + \sum_{j=1, j\neq i}^{N+M} \left(w_{ijx}\dot{e}_{ix} + w_{ijy}\dot{e}_{iy} \right) \right]. \end{aligned} \tag{23}$$

Taking into account Equations 17 the above formula can be transformed to the following form:

$$\frac{dV}{dt} = \sum_{i=1}^{N} \left[E_{ix}\dot{e}_{ix} + E_{iy}\dot{e}_{iy} + e_{i\theta}\dot{e}_{i\theta} \right]. \tag{24}$$

Next, using Equation 21 one obtains:

$$\begin{aligned} \dot{V} = \sum_{i=1}^{N} \left[c_1 E_{ix} e_{iy} e_{i\theta} - c_1 E_{iy} e_{ix} e_{i\theta} - E_{iy} e_{ix} h(t, E_{iy}) + \right. \\ \left. + E_{ix} e_{iy} h(t, E_{iy}) - e_{i\theta} h(t, E_{iy}) - c_1 e_{i\theta}^2 - c_2 E_{ix}^2 \right] \end{aligned} \tag{25}$$

For further analysis a new variable is introduced:

$$\theta_{iE} = Atan2(-E_{iy}, -E_{ix}), \tag{26}$$

the auxiliary orientation variable; function $Atan2(\bullet, \bullet)$ is a version of the $Atan(\bullet)$ covering all four quarters of the Euclidean plane.

Substituting $E_{ix} = D_i \cos\theta_{iE}$ and $E_{iy} = D_i \sin\theta_{iE}$, $D_i = \sqrt{E_{ix}^2 + E_{iy}^2}$ in the above equation one obtains:

$$\begin{aligned} \dot{V} = \sum_{i=1}^{N} \left[c_1 D_i \cos\theta_{iE} e_{iy} e_{i\theta} - c_1 D_i \sin\theta_{iE} e_{ix} e_{i\theta} \right. \\ - D_i \sin\theta_{iE} e_{ix} h(t, E_{iy}) + D_i \cos\theta_{iE} e_{iy} h(t, E_{iy}) \\ \left. - e_{i\theta} h(t, E_{iy}) - c_1 e_{i\theta}^2 - c_2 D_i^2 \cos^2\theta_{iE} \right]. \end{aligned} \tag{27}$$

The above equation can be rewritten as follows:

$$\begin{aligned}\dot{V} = \sum_{i=1}^{N}\Bigg[&-c_1\left(\frac{e_{i\theta}}{\sqrt{2}}+\frac{1}{\sqrt{2}}D_i\sin\theta_{iE}e_{ix}\right)^2\\&-c_1\left(\frac{e_{i\theta}}{\sqrt{2}}-\frac{1}{\sqrt{2}}D_i\cos\theta_{iE}e_{iy}\right)^2-c_2D_i^2\cos^2\theta_{iE}\\&+\left(\sqrt{\frac{c_1}{2}}D_i\sin\theta_{iE}e_{ix}-\frac{h(t,E_{iy})}{\sqrt{2c_1}}\right)^2\\&+\left(\sqrt{\frac{c_1}{2}}D_i\cos\theta_{iE}e_{iy}+\frac{h(t,E_{iy})}{\sqrt{2c_1}}\right)^2\\&-\frac{h^2(t,E_{iy})}{c_1}-e_{i\theta}h(t,E_{iy})\Bigg].\end{aligned}\tag{28}$$

The first three terms in square brackets on the right hand side of Equation 28 are always less or equal to zero. In the next steps remaining terms will be analysed. One can write their sum as follows:

$$\begin{aligned}\dot{V}_r = \sum_{i=1}^{N}\Bigg[&\left(\sqrt{\frac{c_1}{2}}D_i\sin\theta_{iE}e_{ix}-\frac{h(t,E_{iy})}{\sqrt{2c_1}}\right)^2\\&+\left(\sqrt{\frac{c_1}{2}}D_i\cos\theta_{iE}e_{iy}+\frac{h(t,E_{iy})}{\sqrt{2c_1}}\right)^2\\&-\frac{h^2(t,E_{iy})}{c_1}-e_{i\theta}h(t,E_{iy})\Bigg].\end{aligned}\tag{29}$$

Equation 29 can be transformed to the following form:

$$\begin{aligned}\dot{V}_r = \sum_{i=1}^{N}\Big[&D_i^2\frac{c_1}{2}\sin^2\theta_{Ei}e_{ix}^2+D_i^2\frac{c_1}{2}\cos^2\theta_{Ei}e_{iy}^2\\&-D_i\sin\theta_{Ei}e_{ix}h(t,E_{iy})+D_i\cos\theta_{Ei}e_{iy}h(t,E_{iy})\\&-e_{i\theta}h(t,E_{iy})\Big].\end{aligned}\tag{30}$$

The condition $\dot{V}_r \le 0$ is fulfilled if for all i the following inequalities hold true:

$$\begin{aligned}&D_i^2\frac{c_1}{2}\sin^2\theta_{Ei}e_{ix}^2+D_i^2\frac{c_1}{2}\cos^2\theta_{Ei}e_{iy}^2\le\\&\le\left|-D_i\sin\theta_{Ei}e_{ix}h(t,E_{iy})+D_i\cos\theta_{Ei}e_{iy}h(t,E_{iy})\right.\\&\left.-e_{i\theta}h(t,E_{iy})\right|\le D_i\left|\sin\theta_{Ei}\right|\left\|e_{ix}\right\|\left|h(t,E_{iy})\right|\\&+D_i\left|\cos\theta_{Ei}\right|\left\|e_{iy}\right\|\left|h(t,E_{iy})\right|+\left|e_{i\theta}\right|\left|h(t,E_{iy})\right|\\&\le D_i\left|e_{ix}\right|\left|h(t,E_{iy})\right|+D_i\left|e_{iy}\right|\left|h(t,E_{iy})\right|+\left|e_{i\theta}\right|\left|h(t,E_{iy})\right|\end{aligned}\tag{31}$$

that can be rewritten in the compact form as follows:

$$\begin{aligned}&D_i\left\|e_i^*\right\|\left|h(t,E_{iy})\right|+\left|e_{i\theta}\right|\left|h(t,E_{iy})\right|\\&\ge D_i^2\frac{c_1}{2}\left(\sin^2\theta_{Ei}e_{ix}^2+\cos^2\theta_{Ei}e_{iy}^2\right)\end{aligned}\tag{32}$$

where $e_i^* = [e_{ix}\ \ e_{iy}]^T$.

Reduction of the parameter c_1 increases the chances of satisfying inequality (32) that supports stability of the closed-loop system $(\dot{V} \le 0)$. Notice, however, that satisfying $(\dot{V}_r \le 0)$ may not always be possible. In such case stability of the system can be achieved by increasing the value of parameter c_2 (refer to Equation 28). Note that the procedure described in Assumption 3 pushes the robot away from the state where auxiliary orientation variable $\theta_{iE} \cong \pi/2 + \pi d$. In result term $\cos^2\theta_{iE}$ in Equation 28 cannot be arbitrarily close to zero.

The error dynamics (20) with frozen reference signals may be decomposed into two subsystems (Fig. 6). Properties of these subsystems are inherited from the non-collision case described in [7]: the system Σ_1 is uniformly asymptotically stable at the origin, provided that $c_2 > 0$ and ω_i is persistently exciting, globally Lipschitz, and bounded. The origin of the system Σ_2 is exponentially stable if $c_1 > 0$. As a matter of fact, it may also be established that each of these subsystems is input to state stable (ISS). The subsystem $h(t, E_{iy})$ is also uniformly bounded and satisfy $h(t, 0) \equiv 0$. Stability of the origin may be concluded invoking the small-gain theorem for ISS systems [5].

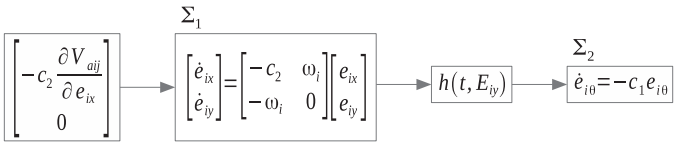

Fig. 6. Diagram of the control system in the collision avoidance mode

If the i-th robot is in the collision avoidance area of the j-th obstacle, but close to its outer edge $(\text{in this case } \|w_{ij}\| \ll \ll \|[e_{ix}\ \ e_{iy}]^T\|)$, collision avoidance terms can be neglected. Correction variables (17) are approximated as follows:

$$E_{ix} \cong e_{ix}, \quad E_{iy} \cong e_{iy}, \tag{33}$$

the algorithm becomes the same as in [7] and the stability analysis presented there is applicable.

In the opposite situation, i.e. for $\|w_{ij}\| \gg \|[e_{ix}\ \ e_{iy}]^T\|$ (i-th robot is close to the boundary of the j-th obstacle, error terms and terms related to collision avoidance with other obstacles are neglected) the correction variables can be approximated in the following way (refer to Equation 17):

$$E_{ix} \cong \frac{\partial V_{aij}}{\partial e_{ix}}, \quad E_{iy} \cong \frac{\partial V_{aij}}{\partial e_{iy}}. \tag{34}$$

When i-th robot is close to the j-th obstacle, in most cases the condition $|E_{ix}| \gg 0$ is fulfilled. The exception is situation when

θ_{iE} is in the neighbourhood of $\pi/2 + \pi d$ (refer to Equation 26). This state is non-attracting, but procedure given in Assumption 3 is applied to push the robot away from this region (if E_{ix} is close to zero linear velocity control v_i is close to zero, refer to Equation 18). Notice that in this case the centre of the obstacle lays close to the axis of the robot wheels (Fig. 7), and thus, application of some arbitrary linear velocity control $\tilde{v}_i$ to the robot does not carry the risk of collision with the j-th obstacle.

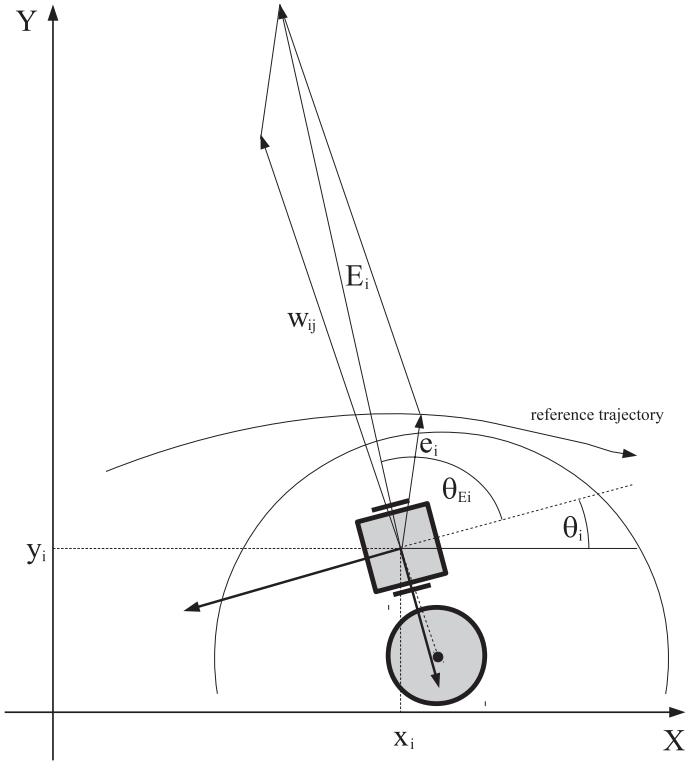

Fig. 7. Robot in the environment with obstacle, $E_{i\theta} = \pi/2$

When the robot is away from this state $\partial V_{aij}/\partial e_{ix}$ has a large value and the boundedness of the output of the collision avoidance subsystem is necessary to prove stability. Substituting first Equation in (17) into first Equation in (21), and using Equations 15 and 16 one can write:

$$\dot{e}_{ix} = h_i(t, E_{iy})e_{iy} + c_1 e_{iy} e_{i\theta} - c_2 e_{ix} - c_2 \frac{\partial V_{aij}}{\partial e_{ix}}. \qquad (35)$$

Note that the above approximation assumes that the robot is located close to the boundary of a single obstacle j, and terms related to the other obstacles are neglected.

If $\partial V_{aij}/\partial e_{ix}$ is sufficiently high (that happens if the robot is very close to the obstacle), i.e. $\partial V_{aij}/\partial e_{ix} \gg e_{ix}$, $\partial V_{aij}/\partial e_{ix} \gg e_{iy}$, $\partial V_{aij}/\partial e_{ix} \gg e_{i\theta}$, and $\partial V_{aij}/\partial e_{ix} \gg h(t, E_{iy})$ the Equation 35 can be approximated as follows:

$$\dot{e}_{ix} \cong -c_2 \frac{\partial V_{aij}}{\partial e_{ix}}. \qquad (36)$$

From the Equation 36 it is clear that $\dot{e}_{ix}$ and $\partial V_{aij}/\partial e_{ix}$ have different sign and as a result $\partial V_{aij}/\partial e_{ix}\dot{e}_{ix} < 0$. To fulfil the condition that $\dot{V}_{aij} = \partial V_{aij}/\partial e_{ix}\dot{e}_{ix} + \partial V_{aij}/\partial e_{iy}\dot{e}_{iy}$ is less then zero the second term on the right hand side must be less then the first one taking their absolute values. This can be obtained by reducing c_1 parameter (refer to Equation 21). The property $\dot{V}_{aij} \leq 0$ guarantees boundedness of both V_{aij} and $\partial V_{aij}/\partial e_{ix}$. Finally one can state that collision avoidance block, that is input to the system shown in Fig. 6, has also bounded output and both error components e_{ix} and e_{iy} in Σ_1 are bounded.

The third considered case is when modules of the position error of the i-th robot and gradient of the collision avoidance function of the j-th obstacle are similar: $\|[e_{ix}\ \ e_{iy}]^T\| \cong \|w_{ij}\|$ (in this case collision avoidance terms of other obstacles are neglected). Both vectors can point in arbitrary directions but one situation is special, if both of them point in exactly opposite directions robot is in the saddle point (Fig. 8). This results in $E_{ix} = 0$ and $E_{iy} = 0$ and, finally, $v_i = 0$ that activates procedure described in Assumption 3. This pushes the robot out of the saddle point usually. The only exception is when the auxiliary orientation variables is $0 + \pi d$ (this is the worst case, robot has the obstacle exactly in the front or exactly at the back and its goal is exactly on the other side of the obstacle; notice that this state is set of measure zero) which can lead to oscillations around the saddle point. In [10] authors of this paper investigated other method of leaving the saddle point. The paper includes extensive tests on real non-holonomic mobile robot.

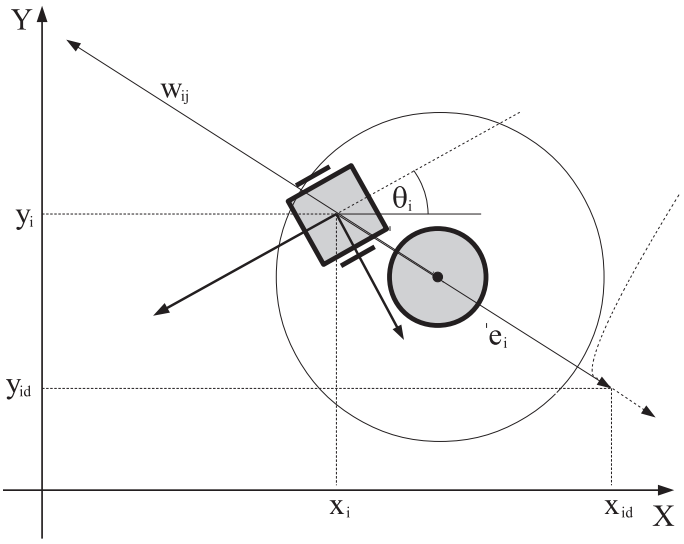

Fig. 8. Robot in the environment with obstacle – saddle point

The above considerations assume that the i-th robot is not located near the boundaries of two or more obstacles at the same time. Taking into account that collision avoidance component of the control is large (close to the obstacle) the robot is driven away quickly and these considerations are correct in most cases. Other situations can be considered exceptional and they are not investigated here.

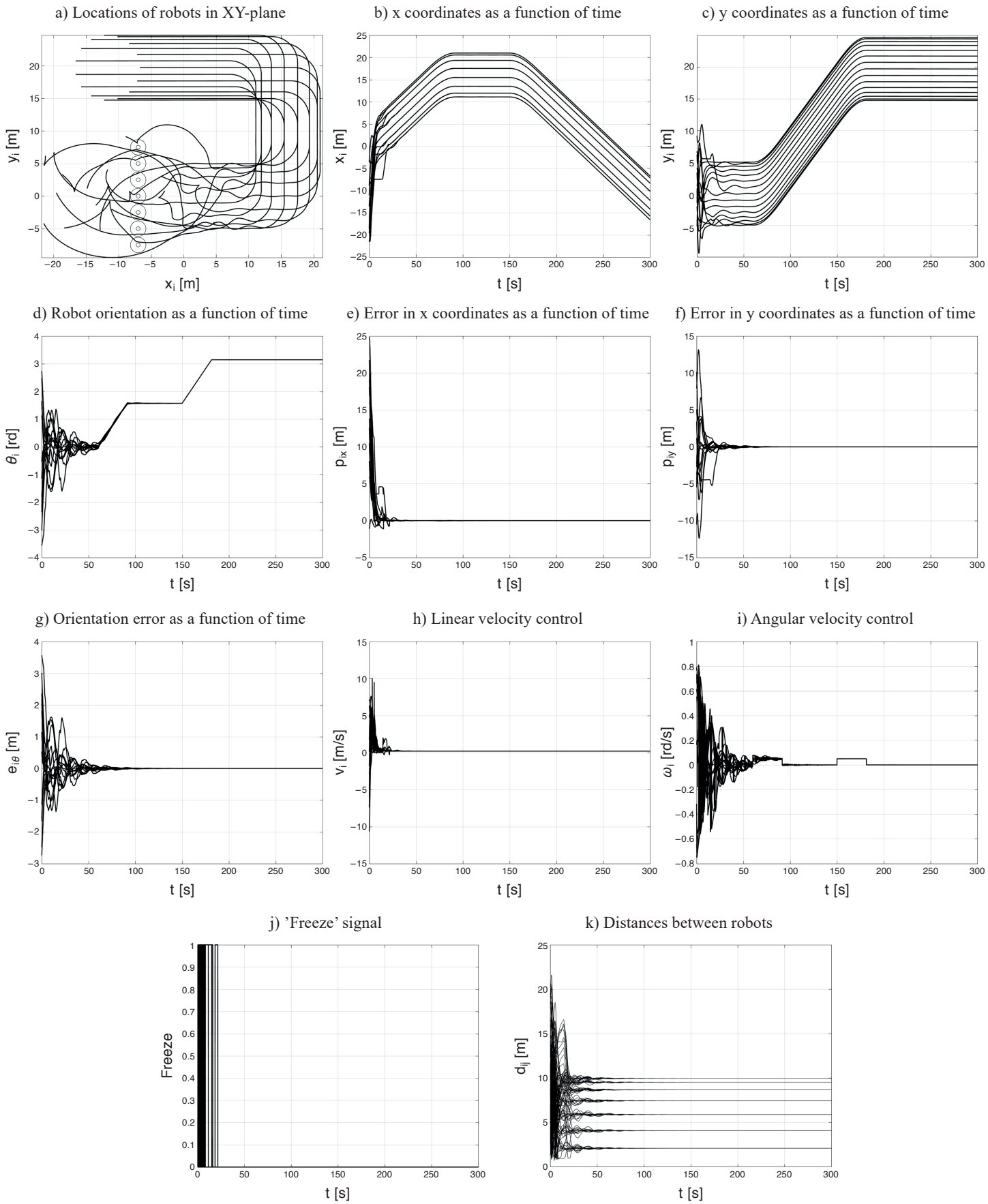

Fig. 9. Numerical simulation: trajectory tracking for $N = 15$ robots

As shown in [8] collision avoidance is guaranteed if $\dot{V}_{aij} \leq 0$ and $\lim_{\|[x_i\ y_i]^\top - [x_j\ y_j]^\top\| \to r^+} V_{aij} = +\infty$, $i \neq j$.

5. Simulation results

In this section numerical simulation for a group of $N = 15$ mobile robots moving in the environment with $M = 7$ static obstacles is presented. Initial coordinates of robots (both positions and orientations) are pseudo-random. The goal is to build ring shaped formation (radius 5 m) moving along straight lines and arcs. Virtual leader is located in the middle of the ring. Initially most of the robots have to pass through a 'barrier' composed of seven static circle shaped obstacles with a diameter $r = 0.3$ m and the range of APF $R = 1.2$ m (the radiuses of robots and the ranges of their APFs are the same). The distances between these obstacles are 2.5 m, there are only 0.1 m wide slots between the neighbouring obstacle APFs. Persistent excitation is $h(t, E_{iy}) = \phi(t)\tanh(E_{iy})$, where function $\phi(t)$ is non smooth pulse function of an amplitude 0.5, period of 4 s and pulse width 80%. It introduces persistent excitation that is necessary to stabilize the system in the y direction.

Virtual leader starts the motion at the origin and initially moves along x axis with linear velocity $v_l = 20$ m/s. After 60 s the angular velocity $\omega_l = 0.05\,^{rd}/_{s}$ is applied still maintaining the previous linear speed. Then, after next 31.4 s its angular velocity is set to zero. Robot is moving straight along y axis for 58.6 s. In the next step angular velocity is set to $\omega_l = 0.05\,^{rd}/_{s}$ and this control is maintained for 31.4 s after which it is set to zero and robot moves along x axis in its negative direction.

The following settings of the algorithm are used: $c_1 = 0.1$, $c_2 = 0.5$, $t_u = 1$ s. In Fig. 9a motion of robots in xy-plane is shown. In Figs. 9b, 9c, 9d time graphs of x_i, y_i and θ_i robots coordinates are presented, respectively. One can see that robots reach their reference signals in about 100 s. In Figs. 9e and 9f position errors expressed in the global coordinate frame are shown. Figure 9g presents orientation errors as a function of time.

In Fig. 9h plots of linear velocity controls are shown. There are peaks several times in the initial state. They appear when robots are near static obstacles. These control values are not realizable in the real systems, and should be scaled down (this will extend the convergence time). In Fig. 9i angular controls for the robots are shown. One can clearly see the sequence of straight motion periods and movement along arcs periods. Figure 9j shows plot of the 'freeze' signals (the reference signals was frozen if this signal is set to 1 and unfrozen otherwise). The periods of 'freezing' reference signal occur for the first 25 s of the transient state. In Fig. 9k relative distances between robots are shown. This graph is not very readable in the initial part because it contains $N(N-1) = 210$ signals, but it is clear that no pair of robots is getting distance close to $2r = 0.6$ m. This minds that no collision occurred.

Visualization of the presented experiment is available on the web page http://wojciech.kowalczyk.pracownik.put.poznan.pl/research/formation-control-persistent-excitation/pe.html.

6. Conclusion

In this paper control algorithm for a group of differentially-driven mobile robots that tracks desired trajectory is presented. Robots avoid collision with each other and other obstacles existing in the taskspace. Stability analysis of the closed-loop system is based on Lyapunov-like function. Simulation results for the formation of 15 robots tracking desired trajectory in the environment with 7 static obstacles show the effectiveness of the algorithm. Authors plan to conduct extensive tests of the proposed control method on a real two-wheeled mobile robots in the near future.

References

[1] G. Leitmann and J. Skowronski, Avoidance Control, *J. Optim. Theory Appl*. 23(4), 581–591, 1977.

[2] G. Leitmann, Guaranteed Avoidance Strategies, *J. Optim. Theory Appl*. 32(4), 569–576, 1980.

[3] K. Do, Formation Tracking Control of Unicycle-Type Mobile Robots with Limited Sensing Ranges, *IEEE Transactions on Control Systems Technology* 16(3), 527–538, 2008.

[4] O. Khatib, Real-time obstacle avoidance for manipulators and mobile robots, *The International Journal of Robotics Research* 5(1), 90–98, 1986.

[5] H. K. Khalil, Nonlinear Systems, 3rd ed. New York, NY, USA, Prentice-Hall, 2002.

[6] A. Loria, E. Panteley, and A.Teel, Relaxed persistency of excitation for uniform asymptotic stability, *IEEE Trans. Autom. Control* (46)12, 1363–1368, December 2001.

[7] A. Loria, J. Dasdemir, and N. Alvarez Jarquin, Leader—Follower Formation and Tracking Control of Mobile Robots Along Straight Paths, *IEEE Transactions on Control Systems Technology* 24(2), 727–732, March 2016, DOI: 10.1109/TCST.2015.2437328.

[8] S. Mastellone, D. Stipanovic, and M. Spong, Formation control and collision avoidance for multi-agent non-holonomic systems: Theory and experiments, *The International Journal of Robotics Research*, pp. 107–126, 2008.

[9] W. Kowalczyk, M. Michałek, and K. Kozłowski, Trajectory tracking control with obstacle avoidance capability for unicycle-like mobile robot, *Bull. Pol. Ac.: Tech*. 60(3), 537–546, 2012.

[10] W. Kowalczyk, M. Przybyła, and K Kozłowski, Saddle point detection of the navigation function in nonholonomic mobile robot control, 21st International Conference on Methods and Models in Automation and Robotics, pp. 936–941, Miedzyzdroje, 2016.

[11] D.V. Dimarogonasa, S.G. Loizoua, K.J. Kyriakopoulos, and M.M. Zavlanosb, A Feedback Stabilization and Collision Avoidance Scheme for Multiple Independent Non-point Agents, *Automatica* 42(2), 229–243, 2005.

[12] I. Filippidis and K.J. Kyriakopoulos, Adjustable Navigation Functions for Unknown Sphere Worlds, *IEEE Conference on Decision and Control and European Control Conference (CDCECC)*, pp. 4276–4281, 2011.

[13] G. Roussos and K.J. Kyriakopoulos, Decentralized and Prioritized Navigation and Collision Avoidance for Multiple Mobile Robots, Distributed Autonomous Robotic Systems – Springer Tracts in Advanced Robotics 83, pp. 189–202, 2013.

[14] G. Roussos and K.J. Kyriakopoulos, Completely Decentralised Navigation of Multiple Unicycle Agents with Prioritisation and Fault Tolerance, *IEEE Conference on Decision and Control (CDC)*, pp. 1372–1377, 2010.
[15] G. Roussos and K.J. Kyriakopoulos, Decentralized Navigation and Conflict Avoidance for Aircraft in 3-D Space, *IEEE Transactions on Control Systems Technology* 20(6), 1622–1629, Novemer 2012.
[16] E. Rimon and D.E. Koditschek, The Construction of Analytic Diffeomorphisms for Exact Robot Navigation on Star Worlds, *Transactions of the American Mathematical Society* 327(1), 71–116, 1991.
[17] E. Rimon and D. Koditschek, Exact Robot Navigation Using Artificial Potential Functions, *IEEE Transactions on Robotics and Automation* 8(5), 501–518, 1992.
[18] W. Kowalczyk, K. Kozlowski, and J.K. Tar, Trajectory tracking for multiple unicycles in the environment with obstacles, 19th International Workshop on Robotics in Alpe-Adria-Danube Region (RAAD 2010), Budapest, 2010, pp. 451–456, DOI: 10.1109/RAAD.2010.5524544.
[19] W. Kowalczyk and K. Kozłowski, Leader-Follower Control and Collision Avoidance for the Formation of Differentially-Driven Mobile Robots, MMAR 2018 – 23rd International Conference on Methods and Models in Automation and Robotics, 27–30 August 2018, Międzyzdroje, Poland.
[20] T. Mylvaganam and M. Sassano, Autonomous collision avoidance for wheeled mobile robots using a differential game approach, *European Journal of Control* 40, pp. 53–61, 2018, https://doi.org/10.1016/j.ejcon.2017.11.005.
[21] I. Harmati and K. Skrzypczyk, Robot team coordination for target tracking using fuzzy logic controller in game theoretic framework, *Robotics and Autonomous Systems* 57(1), 75–86, 2009, https://doi.org/10.1016/j.robot.2008.02.004.
[22] I. Khoufi, P. Minet, M. Koulali, and M. Erradi, "A game theorybased approach for robots deploying wireless sensor nodes," 2015 InternationalWireless Communications and Mobile Computing Conference (IWCMC), Dubrovnik, 2015, pp. 557–562, DOI: 10.1109/IWCMC.2015.7289144.